Progress In Electromagnetics Research M, Vol. 96, 181–190, 2020

An Extended Hybrid Analytical Model for the Shielding Effectiveness Prediction of a Multi-Cavity Structure with Numerous Apertures

Wei Shen[1], Sen Wang[1], Wei Li[1], Hai Jin[2, 3, *], and Hongliang Zhang[2, 3]

Abstract—In this paper, we extend our previously published hybrid analytical model which is for the estimation of shielding effectiveness of a dual-cavity structure with an aperture array to generalize the model for a wider range of applications. In the proposed model, the aperture array in the center, off-center, higher-order modes, and multi-cavity structure are taken into consideration, respectively. At last, a comparison of the results calculated by the extended hybrid analytical model with those obtained by the simulation software CST is given. The results show that the extended hybrid analytical model for the shielding effectiveness prediction of a three-cavity structure with numerous apertures has a higher precision and a higher efficiency.

1. INTRODUCTION

As the electromagnetic environment becomes more and more complex, electromagnetic compatibility has received increasing attention to protect sensitive equipment or reduce electromagnetic leakage. Shielding effectiveness, which is usually abbreviated as SE, is used to estimate the shielding ability of the equipment, which can be expressed as $SE_e = 20\lg|E_{ext}/E_{int}|$ or $SE_m = 20\lg|B_{ext}/B_{int}|$. In order to protect the sensitive electronic equipment from external electromagnetic waves or avoid electromagnetic interference from the electronic components within the system, the shielding cavity especially a multi-cavity system is usually used to increase the shielding effectiveness of electronic equipment in practical applications. In the design process, it is essential to calculate the shielding effectiveness of the multi-cavity system.

Considerable research has been carried out previously to obtain SE, including numerical methods, measurement methods, and analytical methods. Numerical methods have the advantages of high accuracy and can calculate the complex structures, such as method of moments (MoM) [1], finite-element time-domain (FETD) method [2–4], finite-difference time-domain (FDTD) method [5, 6], Baum-Liu-Tesche (BLT) equation [7, 8], and electromagnetic topology [9]. The numerical methods mentioned above are accurate and suitable to predict the SE of complex structures. Despite this, these approaches are either complex or require much computing time. There are also many different measurement methods carried out to obtain SE, such as mode-tuned reverberation chamber, gigahertz TEM cell, and other new methodologies [10–14]. SE can be obtained accurately through experiential measurements. But the measuring platform is expensive and requires repeated measurements. Analytical methods can intuitively estimate the shielding effectiveness of the enclosure of the cavity. Most analytical methods are based on Robinson's circuit models up to now [10, 11], and lots of expansion of Robinson's model have been proposed to solve the electromagnetic shielding rectangular aperture problems [15–23]. Although

Received 12 August 2020, Accepted 8 September 2020, Scheduled 24 September 2020

* Corresponding author: Hai Jin (jinhai@lut.edu.cn).

[1] Sate Grid Shaanxi Electric Power Company Research Institute, 710000, China. [2] College of Electric Engineering and Information Engineering, Lanzhou University of Technology, 730050, China. [3] Key Laboratory of Gansu Advanced Control for Industrial Processes, Lanzhou University of Technology, Lanzhou 730050, China.

there has been much interest in the design of a single cavity or dual-cavity structure with a rectangle enclosure, there have been few studies considering the problem of a multi-cavity structure, especially a three-cavity structure with numerous apertures which is common in practice system.

This paper presents a description of an extended hybrid analytical model for shielding effectiveness prediction of a multi-cavity structure with numerous apertures based on [23]. The rest of this paper is organized as follows. The shielding effectiveness of a multi-cavity structure with numerous apertures is derived in Section 2, including the aperture array in the center and off the center, and the higher-order modes. Section 3 gives the comparison of the results calculated by the extended hybrid analytical model with those obtained by the simulation software CST. Besides, discussions are also drawn in this section. Finally, Section 4 summarizes the results of this paper.

2. ANALYTICAL FORMULATION

2.1. Review of the Previous Hybrid Model of a Dual-Cavity Structure with Numerous Apertures

A dual-cavity structure with an aperture array in the center, an aperture array in an infinite flat plate, and an equivalent circuit are illustrated in Figure 1(a), Figure 1(b), and Figure 1(c), respectively. The definition of parameters can also be seen in Figure 1, in which the incident plane wave is represented by voltage V_0 and impedance $Z_0 = 120\pi\,\Omega$, the enclosure by the shorted waveguide whose characteristic impedance and propagation constant are $Z_g = Z_0/\sqrt{1-(\lambda/2a)^2}$ and $k_g = k_0/\sqrt{1-(\lambda/2a)^2}$ for TE_{10} mode, where $k_0 = 2\pi/\lambda_0$. The enclosure of the cavity and aperture array are equivalent to a short-circuited waveguide and admittance, respectively.

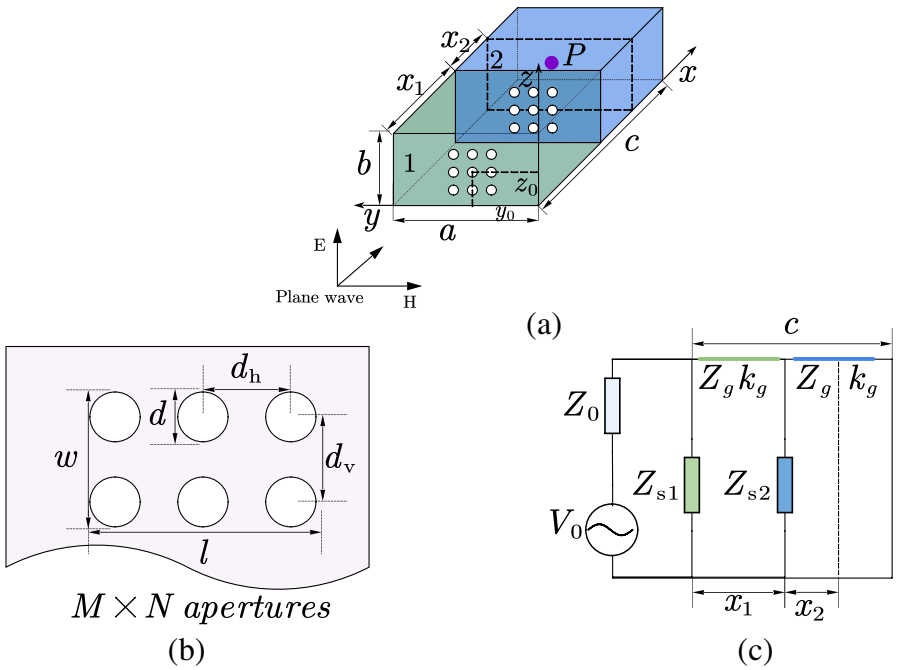

Figure 1. (a) The geometry of a plane-wave irradiating a dual-cavity structure with an aperture array. A dual-cavity structure with dimensions of $a \times b \times c$ and with an $M \times N$ apertures array centered. The monitor point is at the center of the cavity 2. (b) An aperture array in an infinite flat plate. The aperture array is l in length and w in width on the wall, d is the diameter of the hole, d_v and d_h are the vertical and horizontal hole distance, meanwhile, d_v and d_h are larger than d. M and N are the numbers of holes in length and height respectively. (c) Equivalent circuit of the dual-cavity structure with an aperture array.

The aperture array impedance in the finite large cavity is equivalent to admittance given by [18, 19, 23] and can be expressed as

$$Z_s = Z_0 \frac{j\pi d^3}{3d_h d_v \lambda_0} \frac{l \times w}{a \times b} \tag{1}$$

where λ_0 is the free-space wavelength; d is the diameter of holes; d_v and d_h are the vertical and horizontal distances of holes, respectively. Here, it should be noted that Equation (1) is correct only when d_v and d_h are larger than d based on Dehkhoda's model; otherwise, the impedance is incorrect.

Using Thevenin's theorem thrice and the transmission-line theory twice, the equivalent voltage and the source impedance of each layer can be given as Equation (2)∼Equation (7) [23].

$$\begin{cases} V_1 = \dfrac{Z_{s1} V_0}{Z_{s1} + Z_0} \\ Z_1 = \dfrac{Z_0 Z_{s1}}{Z_0 + Z_{s1}} \end{cases} \tag{2}$$

$$\begin{cases} V_L = \dfrac{V_1}{\cos(k_g x_1) + j\dfrac{Z_1}{Z_g}\sin(k_g x_1)} \\ Z_L = \dfrac{Z_1 + jZ_g \tan(k_g x_1)}{1 + j\dfrac{Z_1}{Z_g}\tan(k_g x_1)} \end{cases} \tag{3}$$

$$\begin{cases} V_2 = \dfrac{Z_{s2} V_L}{Z_L + Z_{s2}} \\ Z_2 = \dfrac{Z_L Z_{s2}}{Z_L + Z_{s2}} \end{cases} \tag{4}$$

$$\begin{cases} V_3 = \dfrac{V_2}{\cos(k_g x_2) + j\dfrac{Z_2}{Z_g}\sin(k_g x_2)} \\ Z_3 = \dfrac{Z_2 + jZ_g \tan(k_g x_2)}{1 + j\dfrac{Z_2}{Z_g}\tan(k_g x_2)} \end{cases} \tag{5}$$

$$Z_4 = jZ_g \tan[k_g (c - x_1 - x_2)] \tag{6}$$

$$V_P = \frac{V_3 Z_4}{Z_3 + Z_4} \tag{7}$$

Finally, the electric shielding effectiveness is given by

$$SE_e = 20 \lg \left| \frac{V_P'}{V_P} \right| = 20 \lg \left| \frac{V_0}{2V_P} \right| \tag{8}$$

2.2. Extensions to the Aperture Array Off-Centered

A position factor between the aperture and cavity can be estimated from the enforcing field continuity at the aperture. Based on the waveguide excitation theory, the total modal fields exactly in the aperture (at the excitation point) must correspond to the aperture field. For the excitation of a normal plane wave, the coupling factor can be defined as [21, 22]

$$C_a = \sin\left(\frac{m\pi}{a} y_0\right) \cos\left(\frac{n\pi}{b} z_0\right) \tag{9}$$

Here, m and n are mode indices, and y_0 and z_0 are the positions of the center of the array.

Hence, the impedance of an arbitrarily positioned aperture array can be presented as

$$Z_s' = C_a Z_s = \sin\left(\frac{m\pi}{a} y_0\right) \cos\left(\frac{n\pi}{b} z_0\right) Z_0 \frac{j\pi d^3}{3d_h d_v \lambda_0} \frac{l \times w}{a \times b} \tag{10}$$

Then, replacing Z_s with $Z_s^{'}$, SE_e of the aperture array off-centered can be obtained.

If the aperture array is not circular, such as rectangular or other shapes, the impedance of the aperture array can be replaced by that of an equivalent circle of equal area.

2.3. Extensions to Higher-Order Modes

In the previous hybrid model [23], TE_{10} mode is only considered for most simplified situations. As a matter of fact, higher-order modes may also propagate in the cavity. For this reason, the higher-order modes propagating in the cavity should also be taken into consideration. The characteristic impedance and the propagation constant for TE modes and TM modes can be expressed as Equation (11)∼Equation (13) based on the waveguide theory.

$$Z_{gmn}^{TE} = Z_0 / \sqrt{1 - (m\lambda/2a)^2 - (n\lambda/2b)^2} \tag{11}$$

$$Z_{gmn}^{TM} = Z_0 \sqrt{1 - (m\lambda/2a)^2 - (n\lambda/2b)^2} \tag{12}$$

$$k_{gmn} = k_0 \sqrt{1 - (m\lambda/2a)^2 - (n\lambda/2b)^2} \tag{13}$$

Then we substitute Z_{gmn}^{TE}, Z_{gmn}^{TM}, and k_{gmn} into Eqs. (3)∼(6) for each set of m and n, and the total voltage of point P can be written as

$$V_P = \Sigma V_{P_i} \tag{14}$$

where V_{P_i} is the voltage of the ith set of m and n. So, the electric shielding effectiveness can be given as

$$SE_e = 20 \lg \left| \frac{V_0}{2\Sigma V_{P_i}} \right| \tag{15}$$

2.4. Extensions to Three-Structure Cavity

There may be more than two cavities in the actual electromagnetic system for protecting the sensitive equipment or reducing the electromagnetic leakage. The typical cases are three-structure series-connected and hybrid-connected. The geometry and the equivalent circuit model are shown in Figure 2 and Figure 3. The definition of parameters can also be seen in Figure 2(a) and Figure 3(a).

For series-connection, since the three cavities have the same material, length, and width, $Z_{g1} = Z_{g2} = Z_{g3} = Z_g$, $k_{g1} = k_{g2} = k_{g3} = k_g$. For hybrid connection, the three cavities have different lengths, so the characteristic impedance and propagation constant are not equal anymore, and they can be

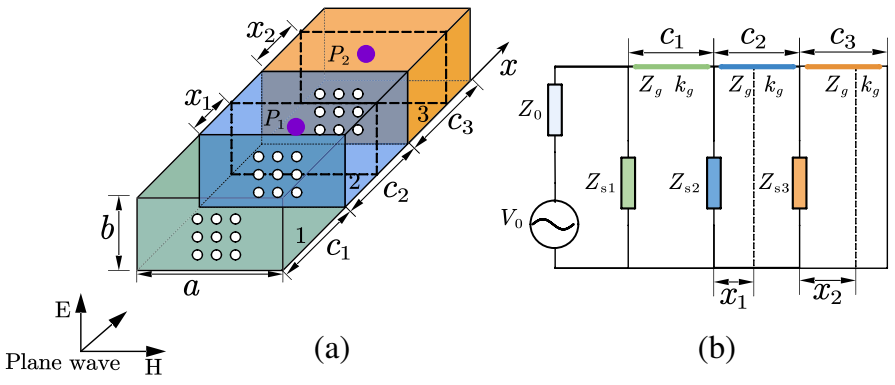

Figure 2. Case 1: The geometry of the three-cavity structure with an aperture array in series-connection (a) three cavities are $a \times b \times c_1$, $a \times b \times c_2$, $a \times b \times c_3$, respectively. Monitor point P_1 and point P_2 are at the center of the cavity 2 and cavity 3 where $x = c_1 + x_1$ and $x = c_1 + c_2 + x_2$, (b) the equivalent circuit model of series-connection.

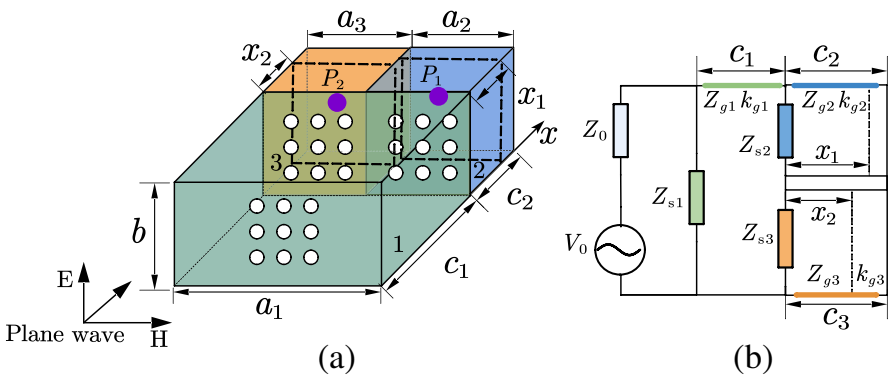

Figure 3. Case 2: The geometry of the three-cavity structure with an aperture array in hybrid connection (a) the three cavities are a in length, b in height, c_1, c_2, and c_3 in width respectively. Point P_1 and point P_2 are at the center of the cavity 2 and cavity 3 where $x = c_1 + x_1$ and $x = c_1 + x_2$, (b) the equivalent circuit model of hybrid-connection.

represented by Z_{g1}, Z_{g2}, Z_{g3}, k_{g1}, k_{g2}, k_{g3} correspondingly. By the same logic with the dual-structure cavity, using Thevenin's theorem four times and the transmission-line theory thrice, we can get the electric shielding effectiveness Equation (16)∼Equation (17) for case 1 and case 2.

$$SE_{eP1} = 20\lg\left|\frac{V_0}{2\sum V_{P_{1i}}}\right| \tag{16}$$

$$SE_{eP2} = 20\lg\left|\frac{V_0}{2\sum V_{P_{2i}}}\right| \tag{17}$$

where i is the index of the set of m and n.

3. NUMERICAL VERIFICATION AND DISCUSSION

To verify the reliability and accuracy of the extended hybrid analytical method presented in Section 2, the results calculated by the analytical method are compared with the CST results under the same parameter conditions. A comparison of two typical structures is considered. The geometry of the three-cavity structure with an aperture array is shown in Figure 2(a) and Figure 3(a). The aperture is a circular hole, and all wall thickness t is 1 mm. Other parameters are given in Table 1. Considering the actual design situation and the convenience of calculation, the frequency bandwidths range from 0 Hz to 2.5 GHz. The monitor probes P_1 and P_2 are at the center of the cavity, where $x_1 = x_2 = 100$ mm.

The electric SE results for case 1 series-connection is shown in Figure 4(a) and Figure 4(b), compared with the result calculated by electromagnetic simulation software CST. The monitor points P_1 and P_2 are the centers of cavity 2 and cavity 3 where the height is 60 mm, and the width is 100 mm.

Table 1. Parameters for the validity of the extended hybrid model.

	Region	Cavity size (mm)			Holes number		Holes size (mm)			Array position (mm)	
		a	**b**	**c**	**M**	**N**	**d**	$\mathbf{d_v}$	$\mathbf{d_h}$	$\mathbf{y_0}$	$\mathbf{z_0}$
Case 1	Cavity 1	300	120	200	5	3	10	20	20	150	60
	Cavity 2	300	120	200	5	3	10	20	20	120	40
	Cavity 3	300	120	200	5	3	10	20	20	180	80
Case 2	Cavity 1	300	120	300	5	3	10	20	20	150	60
	Cavity 2	130	120	200	3	3	10	20	20	85	40
	Cavity 3	170	120	200	5	3	10	20	20	75	80

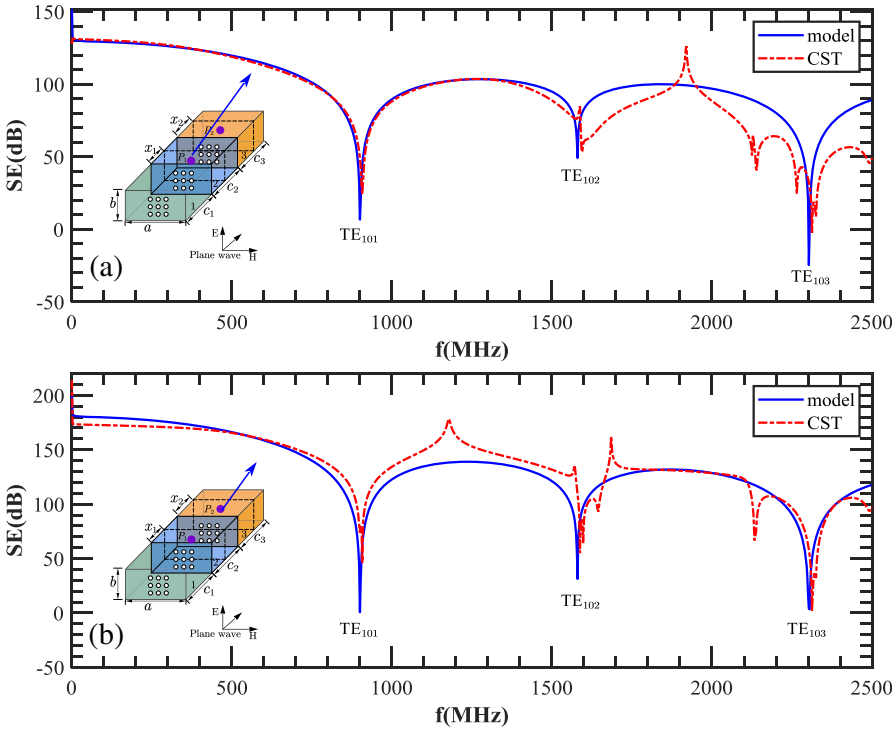

Figure 4. Electric SE results of case 1 in Table 1 obtained by the extended hybrid model and simulation software CST. (a) The electric shielding effectiveness of point P_1 in cavity 2. (b) The electric shielding effectiveness of point P_2 in cavity 3.

All three arrays are 5×3 circles. The diameter of the circle is 10 mm, while the vertical distance and horizontal separations are both 20 mm. Figure 4 shows that results calculated by the extended analytical model are consistent with the CST simulation ones. From Figure 4(a) and Figure 4(b), it is indicated that the resonant frequencies are about 900 MHz (TE_{101} mode), 1580 MHz (TE_{102} mode), 2313 MHz (TE_{103} mode) both in cavity 2 and cavity 3 since the dimensions of the three cavities are the same. The shielding effectiveness of cavity 3 at the resonance frequency is not improved compared to that of cavity 2. The resonance frequency of TE_{103} mode in cavity 2 and cavity 3 should be 2305 MHz according to the size of the structure, but a slight frequency deviation appears at this resonance frequency increased to 2313 MHz, as a result of the increased electrical size of the arrays. The tendency of the presented model results is consistent with that of CST.

The extreme point of the field strength distribution is exactly at the center point of the inner cavity, as shown in Figure 5(a)∼Figure 5(c). Due to the same size of the three cavities, the field strength distribution in the cavity is similar, and the extreme point of the field strength distribution is always at the center of these cavities. According to the calculations, in the frequency range from 0 to 2.5 GHz, it has three resonance frequencies that meet the above conditions, where TE_{101}, TE_{102}, and TE_{103} modes are dominant.

Similarly, the electric SE for case 2 hybrid-connection is shown in Figure 6(a) and Figure 6(b). The monitor points P_1 and P_2 are also at the center of cavity 2 and cavity 3. Their positions are at 60 mm height, 65 mm width, and 60 mm height, 85 mm width, respectively. Cavity 3 changes the number of holes, which is a 3×3 array. The size of the circle is the same as the series-connected one. The calculated results are also in good agreement with the CST results. Not only do the resonant frequencies of cavity 2 and cavity 3 exist, but also the resonant frequency of cavity 1 exists, such as 707 MHz (TE_{101} mode), 1118 MHz (TE_{102} mode), 1581 MHz (TE_{103} mode), and 2060 MHz (TE_{104} mode). It can be seen from Figure 7(a)∼Figure 7(d) that the results prove the correctness of our analytical method once again.

From Figure 4 and Figure 6, the results calculated by our model are in good agreement with that of CST in both series connection and hybrid connection. However, due to the strong electromagnetic field

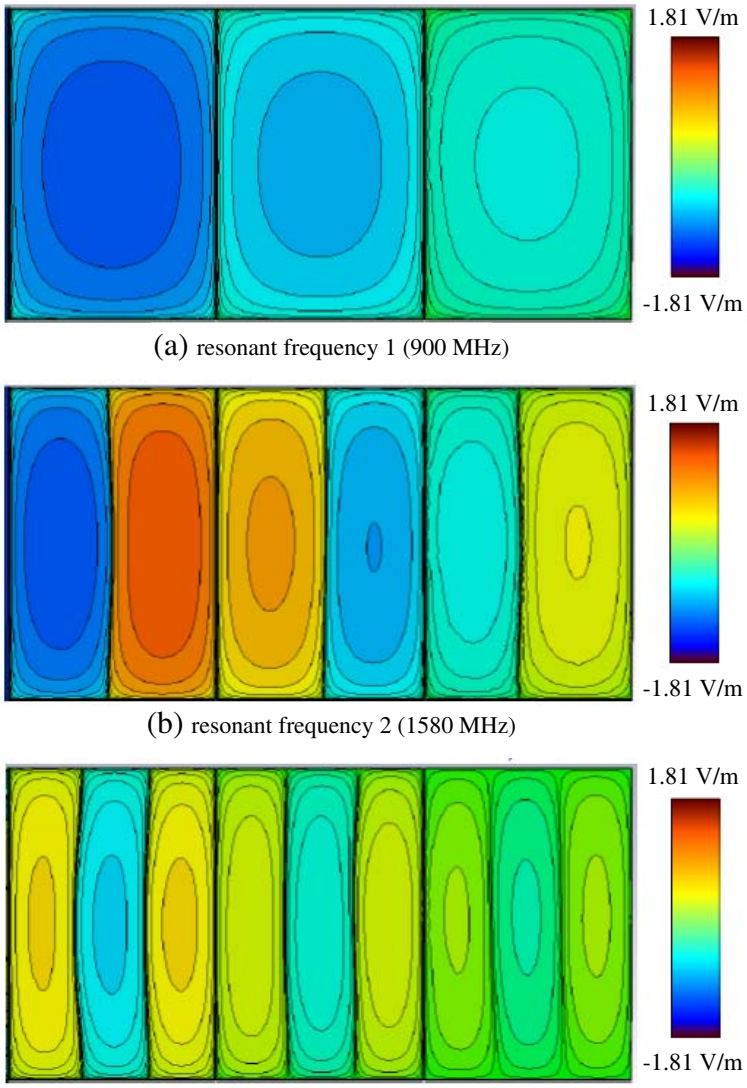

Figure 5. Field distribution of the three-cavity structure for series connection at the different resonance frequency (a) 900 MHz, where TE_{101} mode is dominant, (b) 1580 MHz, where TE_{102} mode is dominant, (c) 2313 MHz, where TE_{103} mode is dominant.

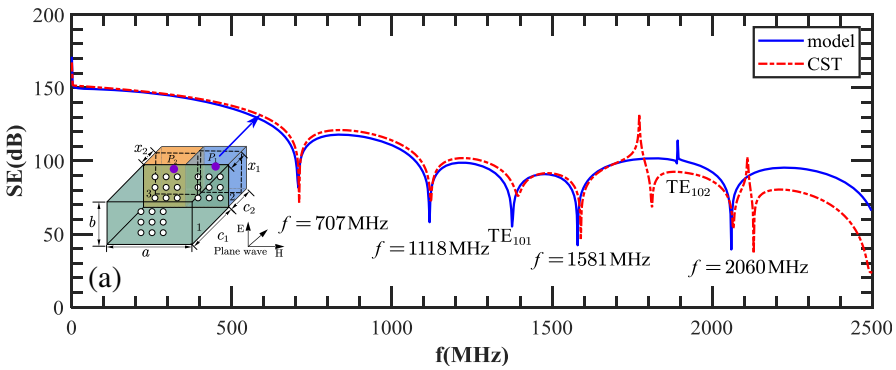

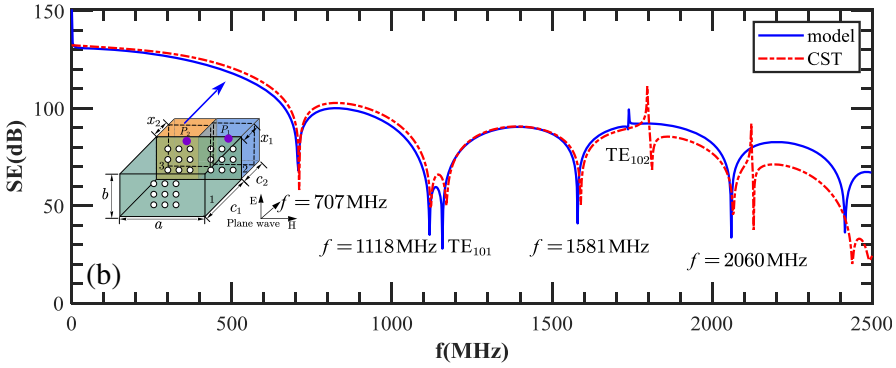

Figure 6. Electric SE results of case 2 in Table 1 obtained by the extended hybrid model, simulation software CST. (a) The electric shielding effectiveness of point P_1 in cavity 2, (b) the electric shielding effectiveness of point P_2 in cavity 3.

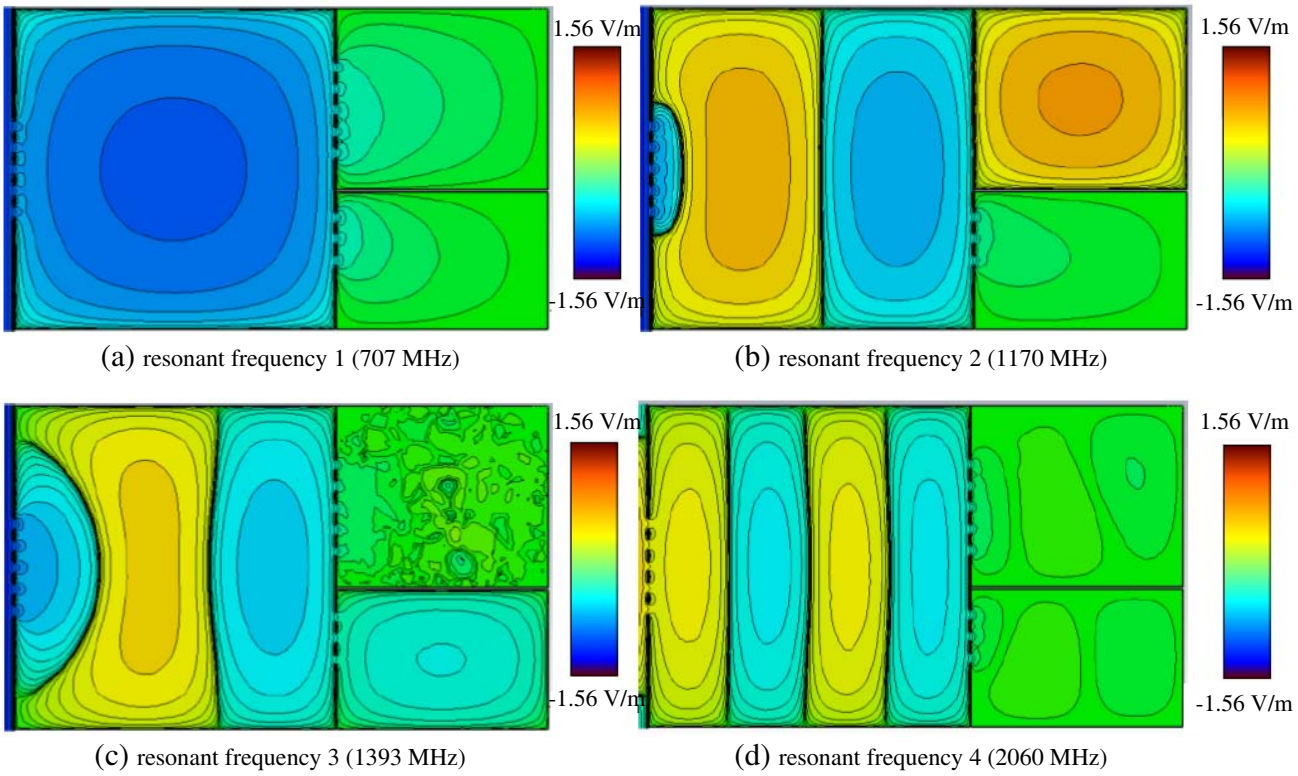

Figure 7. Field distribution of the three-cavity structure for hybrid connection at the different resonance frequency (a) 707 MHz, where TE_{101} mode is dominant of cavity 1, (b) 1170 MHz, where TE_{101} mode is dominant of cavity 3, (c) 1393 MHz, where TE_{101} mode is dominant of cavity 2, (d) 2060 MHz, where TE_{104} mode is dominant of cavity 1.

when the external cavity resonates in a multi-cavity system, the field strength coupled into the internal cavity increases, so the shielding effectiveness of the internal cavity decreases greatly at the resonance point of the external cavity.

The resulting trend of the extended analytical model is consistent with that of the simulation software CST, but the fact remains that a difference still exists at high frequencies. Possible reasons are as follows: (1) We ignored the wall thickness in the presented model because Equation (1) from [18, 19, 23] neglects the wall thickness, but the CST model has wall thickness. It might lead to errors

of increased electrical size of the arrays. (2) It is an approximate calculation that the aperture array of the cavity is regarded as admittance, and it cannot accurately reflect the propagation of electromagnetic fields at high frequency. (3) The centerline of the cavity is at a symmetrical position where the electromagnetic fields cancel out, so the accuracy of the presented model is slightly reduced above 1700 MHz. However, the accuracy of the model is enough for designers to speed up the design process of a multi-cavity structure with numerous apertures, especially where the accuracy is not required strictly. CST takes tens of minutes to analyze the SE while our model gives accurate results in several seconds.

4. CONCLUSIONS

An extended analytical model for an estimation of the shielding effectiveness of the multi-cavity structure is presented in this paper, including the aperture array off-center, higher-order modes, and three-cavity structure. The SE results demonstrate that this extended analytical model is accurate at a wide frequency range, except for a little difference at high frequencies. This method brings convenience to the design of the rectangular shielding cavity in electromagnetic compatibility and the efficient evaluation of the SE of the system.

The verified test to validate our model will be conducted as the further work.

ACKNOWLEDGMENT

This work is supported by National Key R&D Program of China (Project No. 2018YFC0809400), the Project of STATE GRID Corporation of Shaanxi (Project No. 5226KY170010 and No. 2018130), innovation Ability Improvement Project of Colleges and Universities in Gansu Province (2020A-023), and the Foundation of Key Laboratory of Gansu Advanced Control for Industrial Processes, grant number XJ201804 and XJ201808.

REFERENCES

1. Araneo, R. and G. Lovat, "Fast MoM analysis of the shielding effectiveness of rectangular enclosures with apertures, metal plates, and conducting objects," *IEEE Transactions on Electromagnetic Compatibility*, Vol. 51, No. 2, 274–283, 2009.
2. Nie, B.-L. and P.-A. Du, "Electromagnetic shielding performance of highly resonant enclosures by a combination of the FETD and extended Prony's method," *IEEE Transactions on Electromagnetic Compatibility*, Vol. 56, No. 2, 320–327, 2013.
3. Kuo, C.-W. and C.-M. Kuo, "Finite-difference time-domain analysis of the shielding effectiveness of metallic enclosures with apertures using a novel subgridding algorithm," *IEEE Transactions on Electromagnetic Compatibility*, Vol. 58, No. 5, 1595–1601, 2016.
4. Basyigit, I. B., H. Dogan, and S. Helhel, "Simulation of metallic enclosures with apertures on electrical shielding effectiveness," *2017 10th International Conference on Electrical and Electronics Engineering (ELECO)*, 1082–1084, IEEE, 2017.
5. Georgakopoulos, S. V., C. R. Birtcher, and C. A. Balanis, "HIRF penetration through apertures: FDTD versus measurements," *IEEE Transactions on Electromagnetic Compatibility*, Vol. 43, No. 3, 282–294, 2001.
6. Lei, J.-Z., C.-H. Liang, and Y. Zhang, "Study on shielding effectiveness of metallic cavities with apertures by combining parallel FDTD method with windowing technique," *Progress In Electromagnetics Research*, Vol. 74, 85–112, 2007.
7. Baum, C. E., T. K. Liu, and F. M. Tesche, "On the analysis of general multiconductor transmission-line networks," *Interaction Note*, Vol. 350, No. 6, 467–547, 1978.
8. Baum, C. E., "Including apertures and cavities in the BLT formalism," *Electromagnetics*, Vol. 25, Nos. 7–8, 623–635, 2005.
9. Kan, Y., L.-P. Yan, X. Zhao, H.-J. Zhou, Q. Liu, and K.-M. Huang, "Electromagnetic topology based fast algorithm for shielding effectiveness estimation of multiple enclosures with apertures," *Acta Physica Sinica*, Vol. 65, No. 3, 030702–030702, 2016.

10. Robinson, M. P., J. Turner, D. W. Thomas, J. Dawson, M. Ganley, A. Marvin, S. Porter, T. Benson, and C. Christopoulos, "Shielding effectiveness of a rectangular enclosure with a rectangular aperture," *Electronics Letters*, Vol. 32, No. 17, 1559–1560, 1996.
11. Robinson, M. P., T. M. Benson, C. Christopoulos, J. F. Dawson, M. Ganley, A. Marvin, S. Porter, and D. W. Thomas, "Analytical formulation for the shielding effectiveness of enclosures with apertures," *IEEE Transactions on Electromagnetic Compatibility*, Vol. 40, No. 3, 240–248, 1998.
12. Fang, C.-H., S. Zheng, H. Tan, D. Xie, and Q. Zhang, "Shielding effectiveness measurements on enclosures with various aperture by both mode-tuned reverberation chamber and GTEM cell methodologies," *Progress In Electromagnetics Research B*, Vol. 2, 103–114, 2008.
13. Radivojević, M. Vanja, R. Slavko, A. Viktorija, and N. Nataša, "The shielding effectiveness measurements of a rectangular enclosure perforated with slot aperture," *2017 International Conference on Smart Systems and Technologies (SST)*, 121–126, 2017.
14. Shourvarzi, A. and J. Mojtaba, "Shielding effectiveness estimation of a metallic enclosure with an aperture using S-parameter analysis: Analytic validation and experiment," *IEEE Transactions on Electromagnetic Compatibility*, Vol. 59, No. 2, 537–540, 2016.
15. Thomas, D. W., A. C. Denton, T. Konefal, T. Benson, C. Christopoulos, J. Dawson, A. Marvin, S. J. Porter, and P. Sewell, "Model of the electromagnetic fields inside a cuboidal enclosure populated with conducting planes or printed circuit boards," *IEEE Transactions on Electromagnetic Compatibility*, Vol. 43, No. 2, 161–169, 2001.
16. Konefal, T., J. Dawson, and A. Marvin, "Improved aperture model for shielding prediction," *IEEE Symposium on Electromagnetic Compatibility. Symposium Record (Cat. No. 03CH37446)*, 187–192, 2003.
17. Dan, S., Y. Shen, and Y. Gao, "3 high-order mode transmission line model of enclosure with off-center aperture," *International Symposium on Electromagnetic Compatibility*, 361–364, IEEE, 2007.
18. Dehkhoda, P., A. Tavakoli, and R. Moini, "An efficient and reliable shielding effectiveness evaluation of a rectangular enclosure with numerous apertures," *IEEE Transactions on Electromagnetic Compatibility*, Vol. 50, No. 1, 208–212, 2008.
19. Dehkhoda, P., A. Tavakoli, and R. Moini, "Fast calculation of the shielding effectiveness for a rectangular enclosure of finite wall thickness and with numerous small apertures," *Progress In Electromagnetics Research*, Vol. 86, 341–355, 2008.
20. Ren, D., P.-A. Du, Y. He, K. Chen, J.-W. Luo, and D. G. Michelson, "A fast calculation approach for the shielding effectiveness of an enclosure with numerous small apertures," *IEEE Transactions on Electromagnetic Compatibility*, Vol. 58, No. 4, 1033–1041, 2016.
21. Yin, M.-C. and P.-A. Du, "An improved circuit model for the prediction of the shielding effectiveness and resonances of an enclosure with apertures," *IEEE Transactions on Electromagnetic Compatibility*, Vol. 58, No. 2, 448–456, 2016.
22. Shourvarzi, A. and M. Joodaki, "Using aperture impedance for shielding effectiveness estimation of a metallic enclosure with multiple apertures on different walls considering higher order modes," *IEEE Transactions on Electromagnetic Compatibility*, Vol. 60, No. 3, 629–637, 2017.
23. Jin, H., H. Zhang, Y. Ma, K. Chen, and X. Sun, "An analytical hybrid model for the shielding effectiveness evaluation of a dual-cavity structure with an aperture array," *Progress In Electromagnetics Research Letters*, Vol. 91, 109–116, 2020.